

## FREQUENCY-DEPENDENT ATTENUATION IN THE CRUST BENEATH CENTRAL FRANCE FROM $L_g$ WAVES: DATA ANALYSIS AND NUMERICAL MODELING

BY MICHEL CAMPILLO, JEAN-LOUIS PLANTET, AND MICHEL BOUCHON

### ABSTRACT

The quality factor of shear waves in the crust beneath Central France is evaluated by the combined use of data analysis and theoretical modeling. The measurement is made from  $L_g$  wave records of 18 earthquakes at 22 short-period vertical seismic stations of the French seismic network. The geometrical attenuation of  $L_g$  waves has been calculated through a numerical simulation in a perfectly elastic model. The station responses (including site effects) have been evaluated from  $L_g$  waves and from records of the seismic noise.  $Q$  has been calculated for a set of 11 frequencies between 0.5 and 10 Hz and has been found to be in the form

$$Q = 290 * f^{0.52}$$

where  $f$  is the frequency. The numerical simulation leads to the interpretation of  $Q$  of  $L_g$  waves as the mean value of  $Q$  within the crust. Theoretical and experimental decay of energy with distance are in very good agreement. The  $L_g$  waves present a different sensitivity to a low  $Q$  zone whether this zone is associated with the sediments or with scattering in the lower crust. The lower crust beneath central France appears from our experimental results to be associated with high values of  $Q$ .

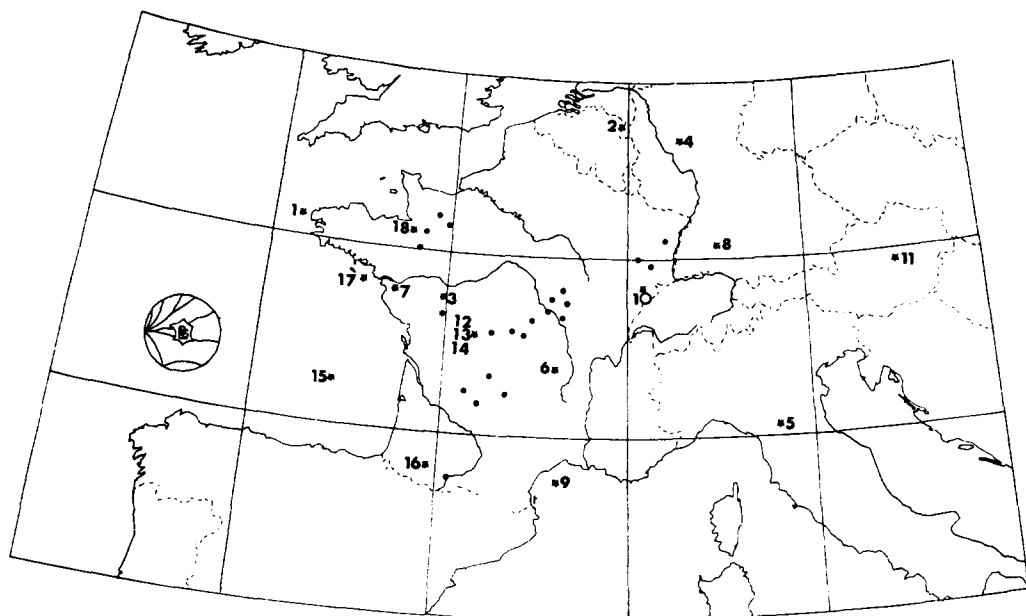
### INTRODUCTION

The most common way to measure the anelastic attenuation of seismic waves in the earth consists in studying the decay of seismic energy with epicentral distance. Interpreted as a superposition of multiply reflected  $S$  waves within the crust, the  $L_g$  wavetrain is particularly well-adapted for attenuation measurement because of its well-constrained domain of propagation (the crust) and its strong amplitude over a large epicentral distance range.

Numerous studies have been done to evaluate the attenuation characteristics of  $L_g$  waves in various regions of world (e.g., Nuttli, 1973; Mitchell, 1975; Bollinger, 1979; Pomeroy and Cheng, 1980; Nicolas *et al.*, 1982). On the other hand, theoretical works have been devoted to the understanding of the excitation, propagation, and geometrical attenuation of  $L_g$  waves in elastic crustal models (Báth and Crampin, 1965; Muller and Mueller, 1979; Bache *et al.*, 1981; Bouchon, 1982; Olsen *et al.*, 1983; Herrmann and Kijko 1983; Campillo *et al.*, 1984). The frequency dependence of  $Q$  of  $L_g$  waves has been evaluated in the United States by Mitchell (1980, 1981). The aim of the present work is to study the frequency dependence of  $Q$  for the crust in central France by combining data analysis with numerical modeling.

### DATA ANALYSIS

In this study, we use the  $L_g$  waves recorded at 22 short-period vertical seismic stations of the French seismic network run by the Laboratory for Detection and Geophysics of the French Atomic Energy Commission. The instruments of this network are described in Nicolas *et al.* (1982). The data set used consists of records from 18 earthquakes located in and around France (Figure 1) and having magnitudes



• STATION  
 15• EARTHQUAKE (The number refers to Table I)

FIG. 1. Locations of the earthquakes and seismic stations used in this study.

TABLE 1  
 LIST OF EVENTS USED IN THIS STUDY

Event No.	Date	Origin Time	Coordinates	$M_L^*$	Region
1†	04/09/81	04h 41 59.2	48.48N 05.11W	4.2	Brest
2†	02/03/82	01h 27 26.3	51.01N 05.77E	4.0	Anvers
3‡	28/05/82	04h 50 24.7	46.98N 00.11W	3.3	La Rochelle
4†	28/06/82	09h 57 33.3	50.69N 07.84E	4.9	Frankfurt
5†	26/07/82	15h 07 29.5	44.26N 10.88E	4.3	Emilie
6‡	08/10/82	13h 19 46.3	45.51N 03.66E	3.3	Clermont-Ferrand
7‡	09/11/82	13h 44 47.3	47.07N 01.73W	3.9	Nantes
8†	28/11/82	04h 34 05.0	48.31N 09.05E	3.9	Jura Souabe
9‡	23/12/82	14h 48 13.4	43.02N 03.75E	4.1	Montpellier
10†	03/02/83	02h 48 30.1	47.34N 06.53E	3.4	Vesoul
11†	14/04/83	14h 52 15.2	47.75N 15.10E	4.8	Salzburg
12‡	21/04/83	01h 53 07.9	46.20N 00.96E	4.0	Bellac
13‡	21/04/83	19h 07 02.1	46.19N 00.98E	3.6	Bellac
14‡	21/04/83	23h 31 13.8	46.20N 00.98E	3.8	Bellac
15†	08/05/83	17h 47 51.4	44.97N 03.47W	4.0	Ouest-Rochefort
16†	06/06/83	01h 29 50.3	43.27N 00.30W	4.1	Pyrenees
17‡	03/07/83	20h 47 11.2	47.21N 02.80W	3.2	L'Orient
18†	07/07/83	03h 52 25.2	48.41N 01.30W	4.2	Fougeres

\*  $M_L$ , local magnitude (LDG).

† CSEM location.

‡ LDG location.

between  $M_L = 3.2$  and  $M_L = 4.8$  (Table 1). The focal depths of these events are not known to have a precision greater than 5 km but they are always located within the crust. If, in general, the ray path from the hypocenter to a station goes through various geological structures, the interstation attenuation measurements relate

exclusively to a relatively stable geological area, namely the Hercynian structure of the Massif Central. The signals are recorded at epicentral distances ranging from 150 to 2000 km. For an individual earthquake, the distance range is more limited because of the dynamics of the instruments (60 dB). The largest distance is about 2 to 3 times the shortest one depending on the frequency band considered. The seismograms are numerically recorded at a sampling frequency of 50 Hz. Figure 2 presents an example of such recordings for the Pyrenean earthquake ( $M_L = 4.1$ ) of 6 June 1983. The epicentral distances lie in this case between 289 and 576 km. The  $Lg$  wavetrain is clearly the prominent phase of the seismograms.

In order to find hypothetical variations of the attenuation, the  $Lg$  wavetrain is separated into three different parts according to their group velocities

$Lg1$ :  $3.6 \text{ km/sec} > V > 3.1 \text{ km/sec}$  (maximum amplitude of  $Lg$ )

$Lg2$ :  $3.1 \text{ km/sec} > V > 2.6 \text{ km/sec}$

$Lg3$ :  $2.6 \text{ km/sec} > V > 2.3 \text{ km/sec}$ .

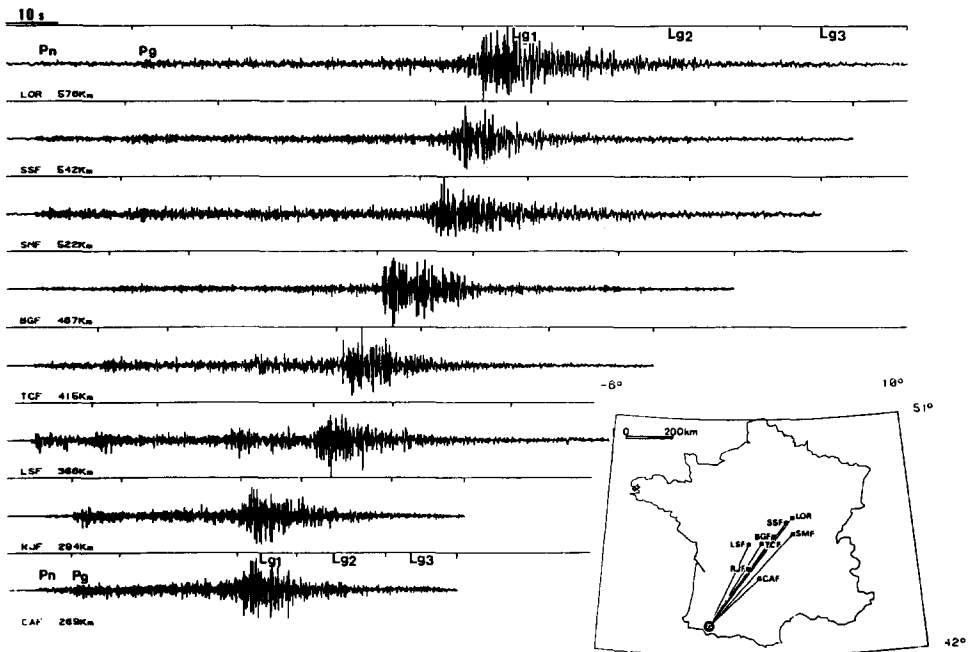


FIG. 2. Examples of seismograms. The epicenter is located in the Pyrenees. The  $Lg$  wave is the prominent phase. Note the three time windows:  $Lg1$ ,  $Lg2$ , and  $Lg3$ .

These group velocities windows are shown in Figure 2 together with those of  $Pn$  and  $Pg$ . For each seismogram, the Fourier spectrum of these three  $Lg$  windows is computed from 0.5 to 15 Hz. The spectrum of the noise during the 30 sec preceding the  $Pn$  arrival is also calculated. The amplitudes of the  $Lg$  wave and of the noise are then compared for all the frequencies and for each phase, and the points at which the signal-to-noise ratio is less than 2 are eliminated. Figure 3 shows an example of  $Lg$  wave spectra for the Pyrenean earthquake of 6 June 1983 whose seismograms are depicted in Figure 2. The spectra of the three segments of the  $Lg$  wavetrain are indicated while the fourth curve represents the noise spectrum. At each station, the shapes of the three phases,  $Lg1$ ,  $Lg2$ , and  $Lg3$  are similar. These spectra, however, widely differ from station to station. Two factors can account for these variations. First, the attenuation may vary with frequency. Second, each

station of the network may be associated with a particular “station response” due to the local geomorphological structure.

The influence of this second factor has to be removed from the data. In order to compute this correction, we shall assume that the inhomogeneity of the station responses acts as a weak perturbation on the decay of spectral amplitude of *Lg* waves. As the signals recorded by the network come from earthquakes located at various epicentral distances, we can evaluate in a statistical way a mean value of the attenuation of the *Lg* wave amplitude for each frequency.

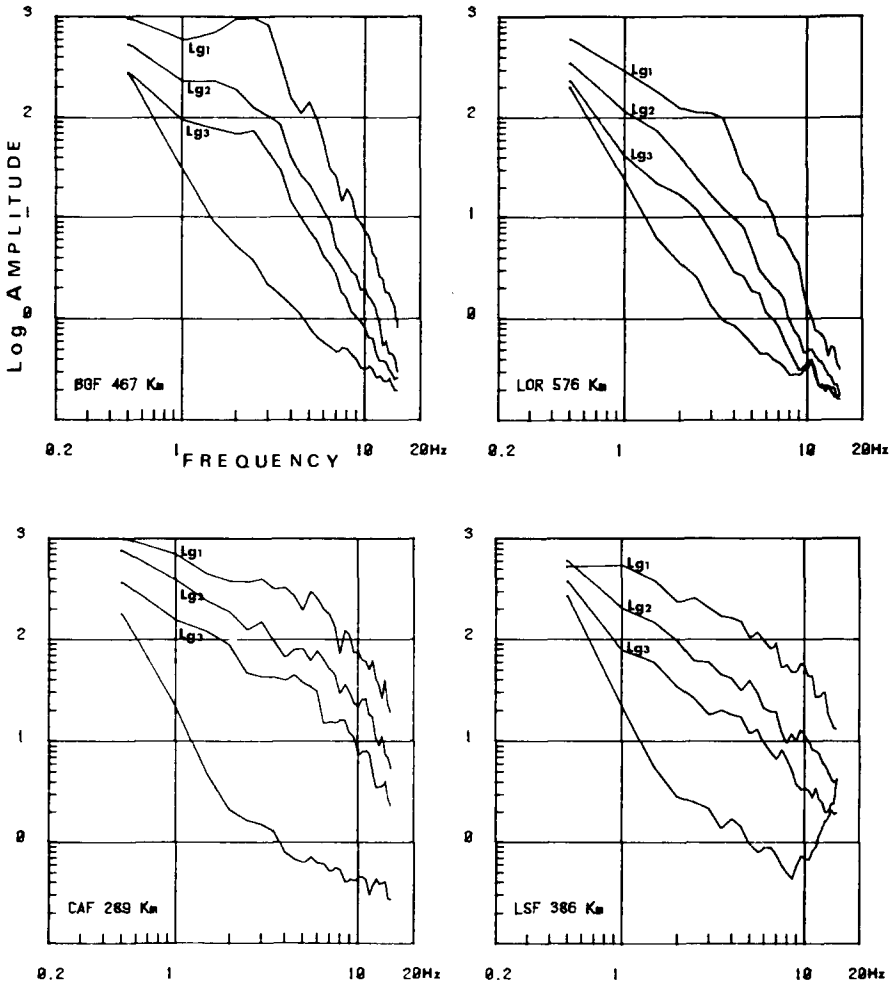


FIG. 3. Examples of spectra of the three phases (*Lg*1, *Lg*2, and *Lg*3) corresponding to the seismograms presented on Figure 2. The unlabeled curve represents the spectrum of the noise.

### SIMULTANEOUS EVALUATION OF THE STATION RESPONSE AND THE QUALITY FACTOR

We denote by *A* the spectral amplitude of the *Lg* wave in a given group velocity window divided by the window length. We can write the spectral amplitude *A* of the *Lg* wave at station *i* produced by earthquake *j* in the approximative form

$$A_{ij}(f, d) = S_j(f) * E(d) * AA(f, d) * ST_i(f) \tag{1}$$

where  $d$  denotes the epicentral distance,  $f$  the frequency and

$S_j(f)$  = the source excitation. We neglect here the azimuthal dependence of the radiation pattern.  $S_j(f)$  is thus mainly dependent on the magnitude.

$E(d)$  = the geometrical spreading of the  $Lg$  wave in the time domain and is of the form

$$E(d) = d^{-0.83}. \quad (2)$$

As we have shown in a previous study (Campillo *et al.*, 1984)

$AA(f, d)$  = the term of anelastic attenuation and can be expressed in the form

$$AA(f, d) = e^{-df/VQ(f)} \quad (3)$$

where  $V$  denotes the  $Lg$  wave group velocity and  $Q(f)$  is the quality factor of shear waves at frequency  $f$ .

$ST_i(f)$  = the station response and represents the particular characteristics of the station which are not described by the standard instrumental response of the network. We further assume that

$$\prod_{i=1}^N ST_i(f) = 1. \quad (4)$$

where  $N$  is the number of stations.

Equation (1) is solved by an iterative process

- (a) We first take  $ST_i(f) = 1$  and we evaluate  $S_j(f)$  and  $Q(f)$  by least squares for each earthquake and each frequency.
- (b) We combine the results of (a) and calculate  $Q(f)$  for the entire set of earthquakes. We assume it to be of the form

$$Q(f) = Q_0 * f^b. \quad (5)$$

- (c) We compute the perturbations to give the transfer functions of the stations. The "station response" is given for each frequency by the mean value of the observed residues at this station for the entire set of earthquakes. This calculation is done under the hypothesis expressed by equation (4). This process is stable and converges in a few iterations. The station responses obtained are shown by solid lines in Figure 4. Most of them are relatively flat for frequencies less than 5 Hz.

As a test of accuracy of these results, we have calculated the station responses to the seismic noise. We assume that the noise is stationary over the entire set of stations used in this study. This hypothesis is strictly valid only in the frequency range from 1 to 5 Hz. We have calculated at each station the ratio between the noise observed and the mean value of the noise recorded on the network. These curves are plotted with dashed lines in Figure 4. The good correlation between the

two types of curves of Figure 4 shows the physical validity of the corrections that we apply to the data.

The iterative resolution of equation (1) leads simultaneously to the station response and to the regional value of  $Q(f)$ . The results for the attenuation are presented in Figure 5. The mean quality factors obtained for the three  $Lg$  groups are

$$\begin{aligned}
 Q &= (290 \pm 80) * f^{(0.52 \pm 0.1)} \\
 Q &= (295 \pm 80) * f^{(0.55 \pm 0.1)} \\
 Q &= (350 \pm 90) * f^{(0.5 \pm 0.1)}.
 \end{aligned}
 \tag{6}$$

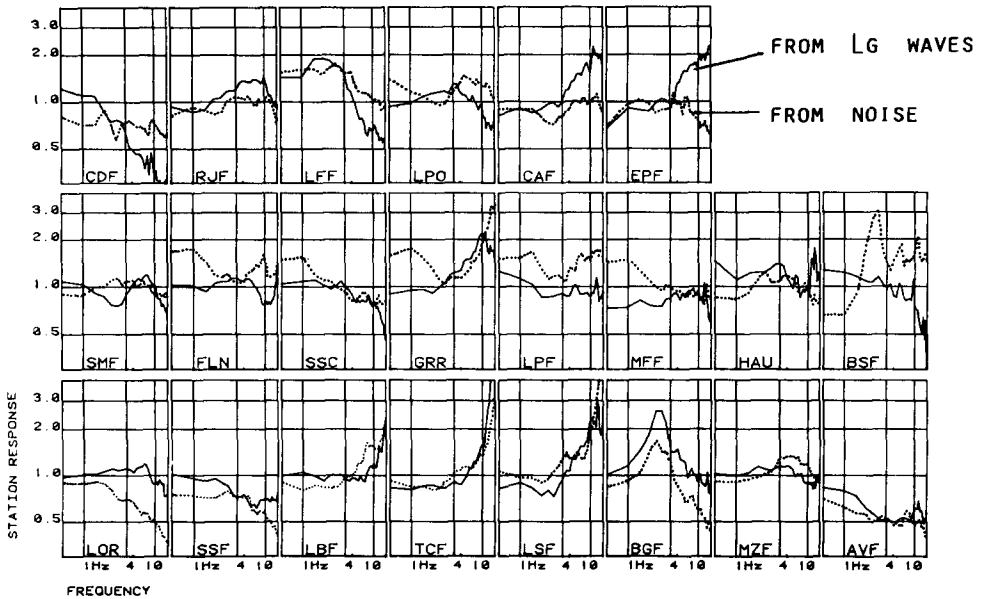


FIG. 4. Station responses of the stations of our network. The responses are calculated from  $Lg$  waves (solid line) and from the seismic noise (dotted line).

If we constrain  $b$  to be the same for the three groups, we get

$$Q = Q_0 * f^{0.52}$$

with

$$Q_0 = 290 \text{ for } Lg1$$

$$Q_0 = 310 \text{ for } Lg2$$

$$Q_0 = 330 \text{ for } Lg3.$$

These relations show that the quality factors measured for the three phases that we have defined in the  $Lg$  wavetrain are very close and thus indicate that the physical processes responsible for this attenuation are the same for the three phases.

NUMERICAL MODELING OF  $Lg$  WAVE ATTENUATION

We now use theoretical modeling to show that  $Q$  of  $Lg$  is an effective measurement of  $Q_s$ , the mean value of the quality factor of shear waves in the crust. The crustal model that we use was inferred from long-range refraction experiments in central

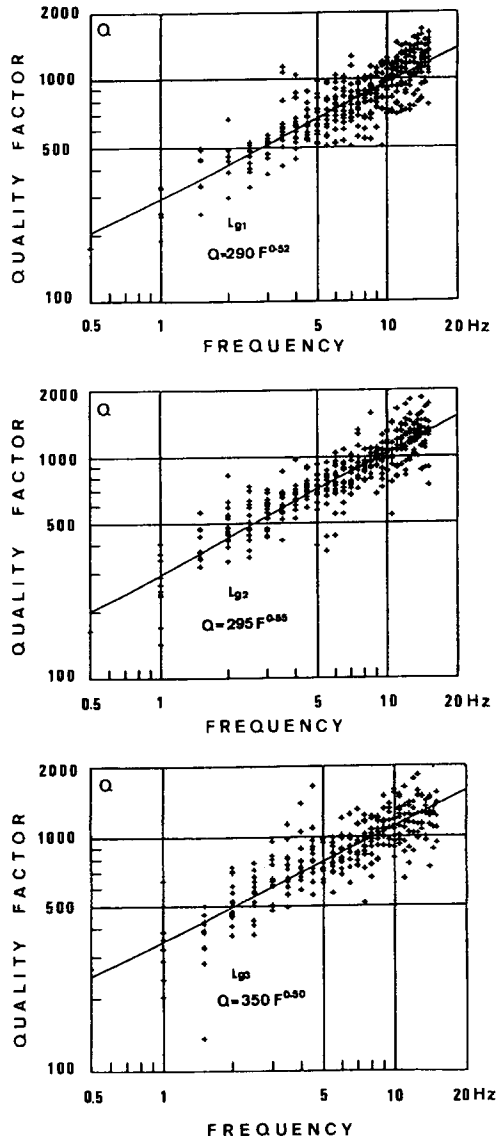


FIG. 5. Frequency-dependent quality factor calculated from our data for the three phrases ( $Lg1$ ,  $Lg2$ , and  $Lg3$ ).

France (Perrier and Ruegg, 1973) and is given in Table 2. It consists of a four-layer crust overlying a mantle half-space. We take as intrinsic quality factor for shear waves the quality factor experimentally obtained for  $Lg$  waves, i.e.,

$$Q_s = 290 * f^{0.52}.$$

For  $P$  waves, we assume  $Q_p = 2*Q_s$ . The calculations are done using the discrete radial wavenumber representation of the seismic field (Bouchon, 1981). The source considered is a point of vertical strike-slip dislocation at a depth of 10 km. The calculations are done for epicentral distances ranging from 180 to 700 km, and the results are shown in Figure 6 where they are compared to the case of a perfectly elastic crust. The seismograms represent the vertical component of the crustal response to a sudden step-function dislocation. The frequency range extends from

TABLE 2  
CRUSTAL MODEL

Layer Thickness (km)	P-Wave Velocity (km/sec)	S-Wave Velocity (km/sec)	Density (gm/cm <sup>3</sup> )
2	4.5	2.6	2.6
16	6.0	3.5	2.8
6	6.3	3.65	2.9
6	6.7	3.9	3.1
	8.2	4.7	3.3

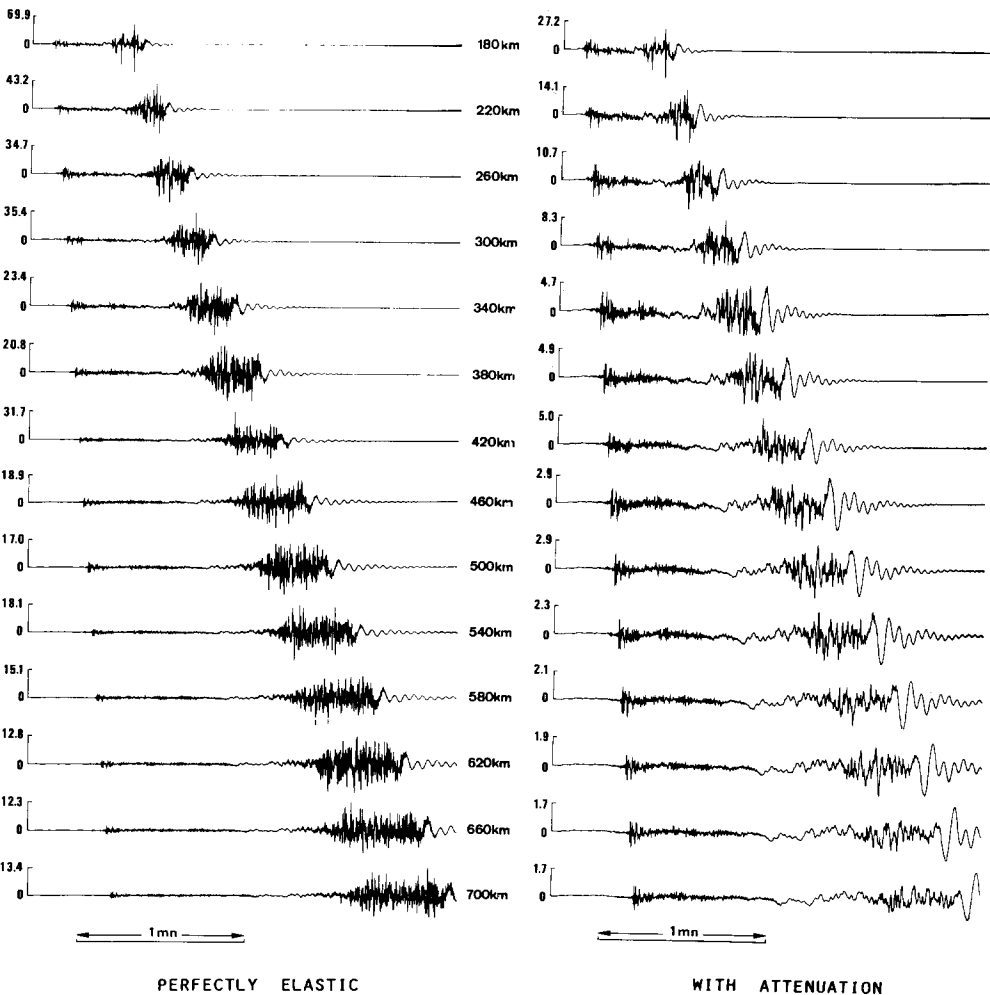


FIG. 6. Synthetic seismograms calculated in a perfectly elastic medium and after introduction of anelastic attenuation.



0 to 5 Hz. The attenuation strongly affects the waveforms and the amplitudes and results in an enhancement of *Pg* waves and Rayleigh waves relative to the *Lg* wavetrain.

The corresponding theoretical *Lg* wave spectra are presented in Figure 7. They are computed over a time window corresponding to group velocities between 3.8 and

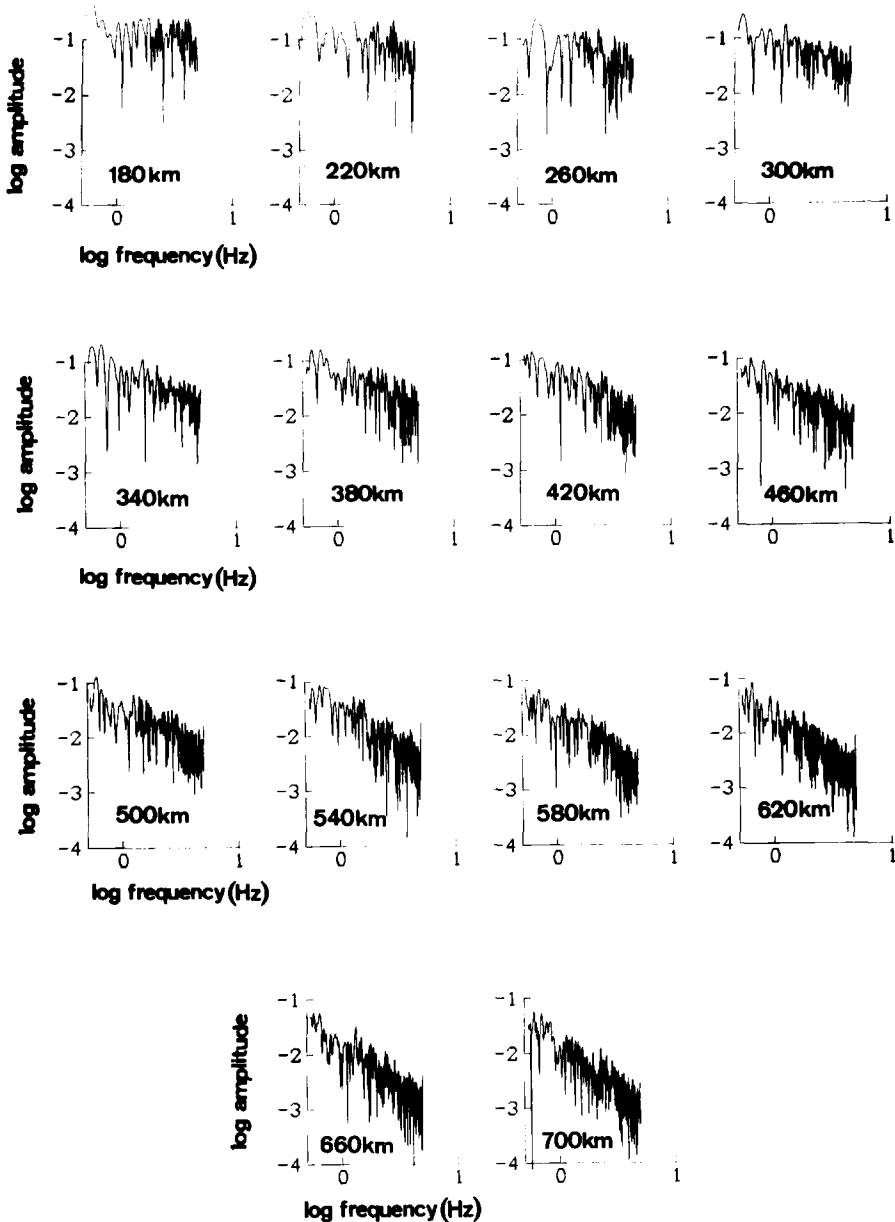


FIG. 7. Evolution of the spectra of *Lg* waves with distance in the presence of anelastic attenuation.

2.5 km/sec. The attenuation of the high frequencies with increasing epicentral distance is clearly visible. At 180 km, the effect of attenuation is small and the *Lg* wave spectrum is almost flat. This is in agreement with the results obtained by Herrmann and Kijko (1983) who showed by using higher mode surface wave theory that the spectrum of the *Lg* wave transfer function for an elastic crust is approxi-

matively flat for frequencies up to 10 Hz. This differs from a result we reported earlier (Campillo *et al.*, 1984) and which was due to an incomplete evaluation of the wavenumber series for large horizontal wavenumbers at high frequency. From the results of Figure 7, we can infer the amplitude fall-off with distance at various frequencies. The numerical results obtained are compared with the data in Figure 8. We have selected in the dataset the earthquakes whose corner frequency is greater

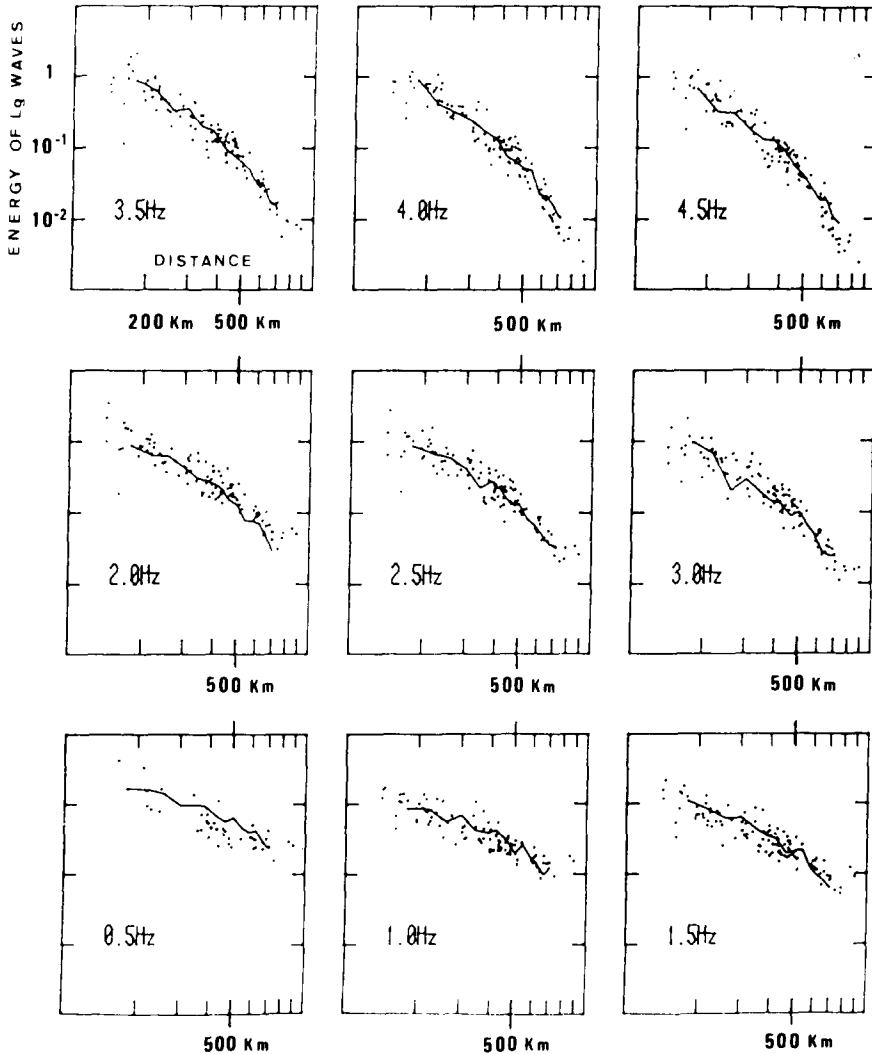


FIG. 8. Decay of spectral energy of *Lg* waves with distance for different frequencies. Comparison between numerical simulation (solid line) and observed points.

than 5 Hz, and we have normalized the theoretical spectra so that the mean values (in the least-squares sense) of the observed and synthetic spectra at 180 km are equal. The comparison with the data shows a very good agreement between observations and calculations which supports the interpretation of *Lg* wave attenuation as a shear-wave crustal attenuation. These results demonstrate the accuracy of numerical modeling in evaluating the energy and the spectral characteristics of seismic waves. A simple flat layer crustal model with a frequency-dependent quality

factor leads to a very realistic simulation of  $Lg$  waves both in the time domain as shown by Bouchon (1982) and in their spectral content as demonstrated here.

The effect of the source depth and the distribution of  $Q$  within the crust on the attenuation of  $Lg$  waves can be investigated by ray tracing. As  $Lg$  waves are made

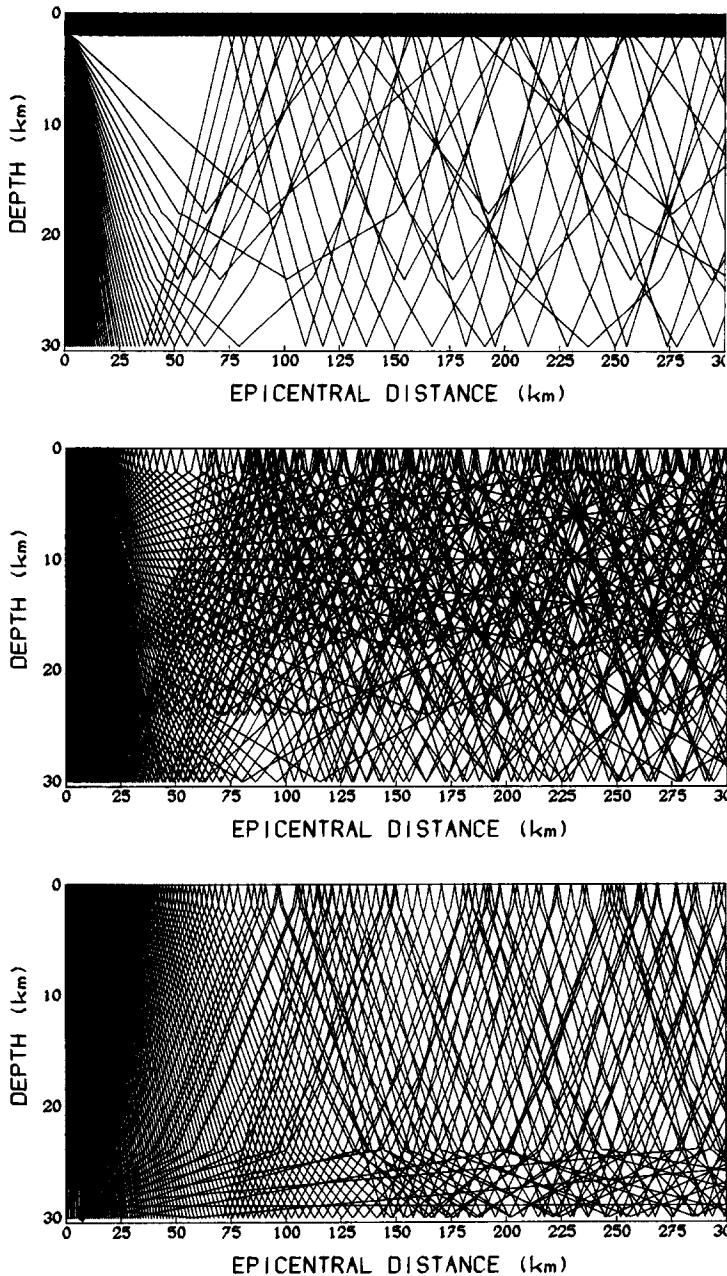


FIG. 9. Supercritically reflected rays radiated by sources at 0-, 10-, and 29-km depth. This tracing illustrates the different samplings of the crust by  $Lg$  waves produced by earthquakes at different depths.

up of multiple supercritically reflected  $S$  waves, the shear-wave velocity in the source region should strongly affect their propagation. An illustration of this dependency is presented in Figure 9. We have drawn on this figure all the supercritically reflected rays (i.e., the individual contributions to the  $Lg$  wavetrain)

radiated by sources located at 0, 10, and 29-km depth. Clearly, the  $L_g$  waves radiated by the three sources sample with different weight different regions of the crust. A deeper source will sample the crust more uniformly than a source located in the upper crust. The examples of the two shallowest sources show that the rays which

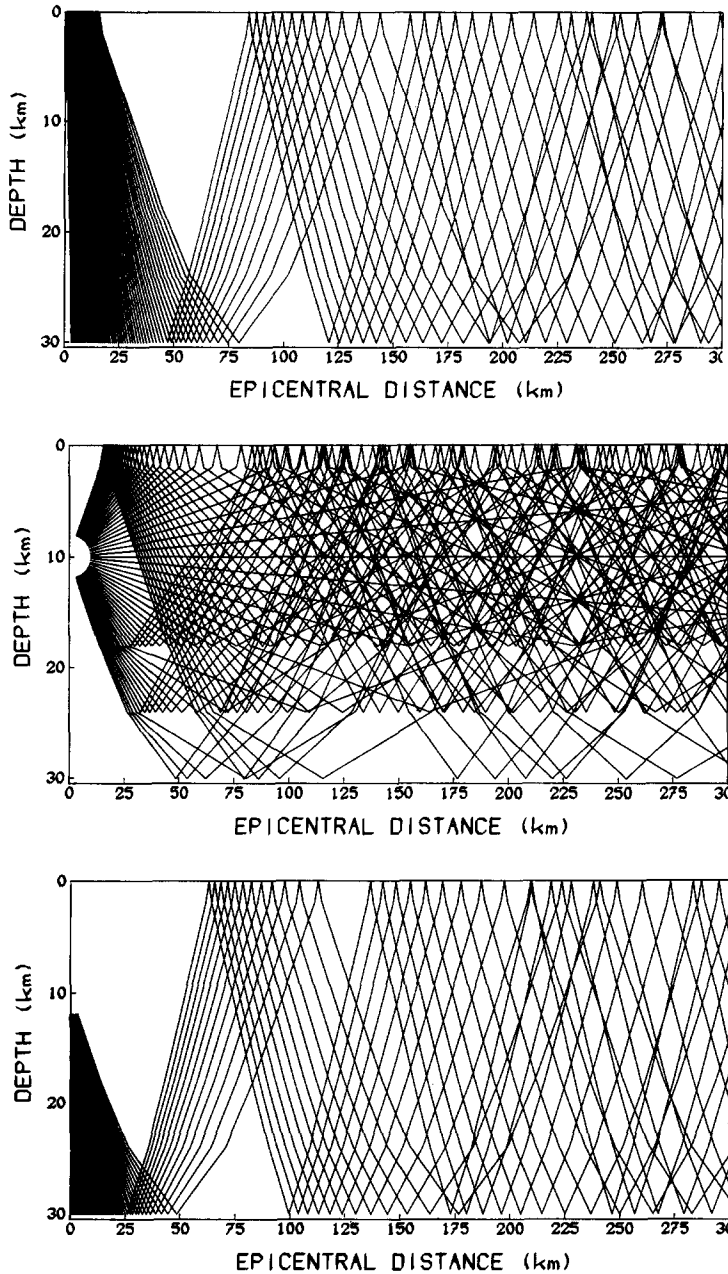


FIG. 10. Supercritically reflected rays radiated by a source at 10-km depth in three different ranges of take-off angles:  $0^\circ$  to  $60^\circ$  (top);  $60^\circ$  to  $120^\circ$ ;  $120^\circ$  to  $180^\circ$  (bottom).

contribute to the  $L_g$  wavetrain are supercritically reflected on the different discontinuities of the crust.

Another related phenomenon is depicted in Figure 10. We have traced there all the supercritically reflected rays radiated by a 10-km deep source and leaving the

source in three different ranges of take-off angles:  $0^\circ$  to  $60^\circ$ ;  $60^\circ$  to  $120^\circ$ , and  $120^\circ$  to  $180^\circ$ . The near-horizontal rays do not sample the lower crust while the more oblique ones which are associated with longer travel times sample the crust quite uniformly.

These simple calculations bring to our attention the problem of knowing which zone of the crust is sampled by  $L_g$  waves for a given earthquake and a given group velocity. In order to further investigate this problem, we have studied the sensitivity of  $L_g$  waves to a zone of strong attenuation in different regions of the crust. We

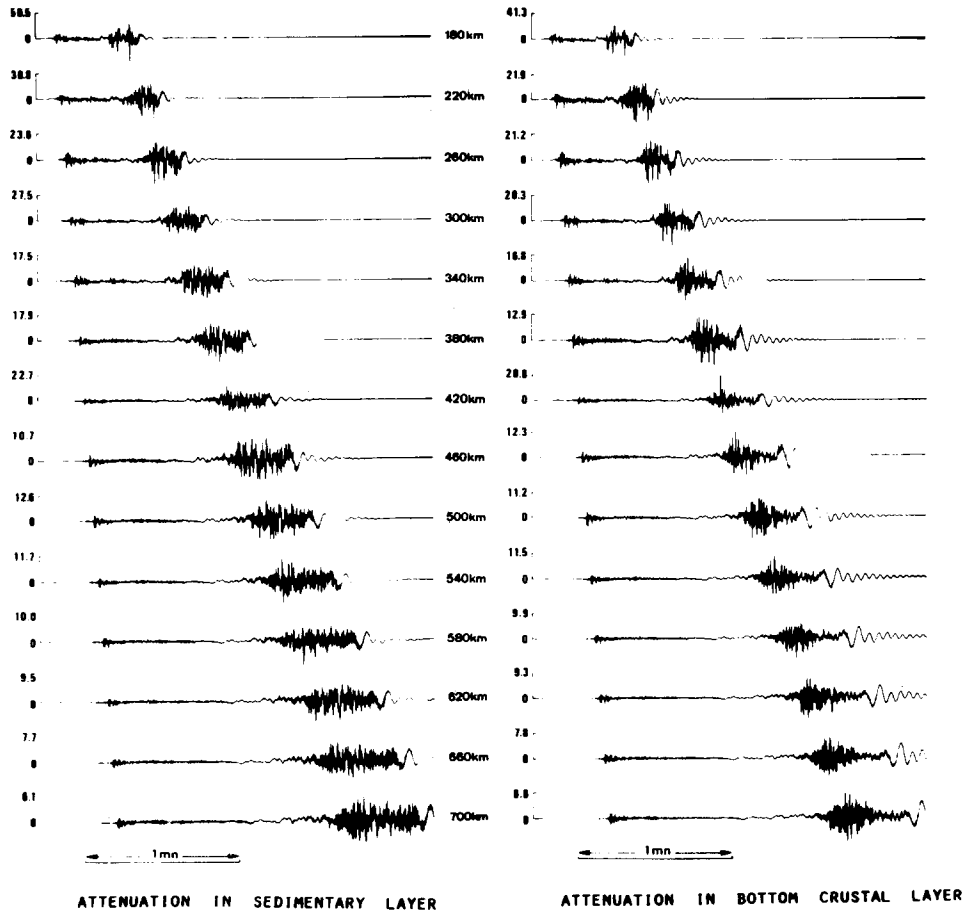


FIG. 11. Synthetic seismograms calculated for crustal models where all the attenuation occurs in the sediments (*left*) and in the lower crust (*right*).

first investigate the effect of a low  $Q$  in the sedimentary layer. We present in Figure 11 (*left*) a profile of synthetic seismograms computed for the crustal model previously used (Table 2), but we assume that all the attenuation occurs in the upper 2 km of the crust and is of the form

$$Q_s = 100 * f^{0.5}$$

These synthetics show that the high frequencies attenuate only slightly with distance and suggest that a zone of low  $Q$  in the sediments or at shallow depth has little effect on the  $L_g$  wavetrain with respect to the results of the perfectly elastic case (Figure 6, *left*).

It is also interesting to investigate the effect of a zone of high attenuation at the base of the crust. For this purpose, and in order to separate such effects, we consider a model where all the attenuation occurs in the bottom crustal layer. We again assume in this layer (the last crustal layer in Table 2)

$$Q_s = 100 * f^{0.5}.$$

The resulting seismograms are presented in Figure 11 (right). In spite of different apparent  $Q$  values for the last two models considered, the maximum amplitudes of  $Lg$  are quite similar. The seismograms computed in the presence of an attenuating zone in the lower crust show a sharp attenuation of the  $Lg$  wave coda. The comparison with Figure 11 (left) is particularly striking in this respect: the  $Lg$  wave coda is quite insensitive to the presence of highly attenuating sediments but will be strongly affected by attenuation or scattering at the base of the crust. This suggests that it is possible to extract more information from the data by evaluating  $Q$  for different parts of the  $Lg$  wavetrain. This is what we have attempted in the first part of this paper by considering three different time windows  $Lg1$ ,  $Lg2$ , and  $Lg3$ . The results inferred, namely a weak increase of the quality factor with decreasing group velocity, indicate that the quality factor of the lower crust is greater than the mean value of  $Q$  in the crust. In particular, these results suggest that the crust-mantle transition beneath central France is a relatively laterally homogeneous discontinuity because there is no evidence for the presence of a zone of strong scattering near the Moho in our data. The attenuation of  $P$  waves in the upper crust of Massif Central has been evaluated by Thouvenot (1983) by using deep seismic sounding data.  $Q_p$  was found to increase almost linearly with depth. The values of  $Q_p$  given by Thouvenot (from 40 close to the surface up to 600 at 7-km depth for a frequency of 20 Hz) indicate that the associated  $Q_s$  values in the upper crust are smaller than the mean value we have obtained. All these results point to an increase of  $Q_s$  with depth in the crust beneath central France.

#### DISCUSSION

We have inferred a value of about 290 as the mean quality factor in the crust at a frequency of 1 Hz. This finding may be compared with the results obtained in different regions of the world. In young tectonic provinces, the values reported show a strong attenuation. In California values of 80 (Aki and Chouet, 1975), 150 (Singh and Hermann, 1983) and 200 (Nuttli, 1982) have been reported. Low values have been found in Asia, 64 in Iran (Nuttli, 1980), 90 for the southern border of USSR (Nuttli, 1981), and 100 in the Garm region (Roecker *et al.*, 1982). Studies in Japan indicate a value around 100 (Aki, 1980). From Alaskan earthquake data, Biswas and Aki (1984) have found  $Q$  to be roughly 150. In stable regions, higher values have been inferred: from about 200 in central and western Asia (Nuttli, 1981) to 450 in Eastern North America (Nuttli, 1973; Bollinger, 1979) and up to 1350 (Singh and Herrmann, 1983) and 1500 (Nuttli, 1982) in the Central United States.  $Q_s$  for central France appears to be a median value between the ones typical of active and stable regions. Geologically, the Massif Central is a tabular Hercynian structure which has been only slightly affected by the alpine orogenesis.

From a compilation of the different evaluations of  $Q$  in the lithosphere from  $S$  waves or coda waves in the frequency range from 1 to 10 Hz (for references see Sato, 1984), the functional dependence of  $Q$  with frequency has been found to be in

the form

$$Q(f) = Q_0 * f^n \quad \text{with } n \text{ varying from 0.3 to 1.}$$

Young tectonic provinces like Japan (Aki and Couet, 1975; Aki, 1980) or California (Aki and Chouet, 1975; Singh *et al.*, 1981; Nuttli, 1981) are associated with values of  $n$  in the range from 0.6 to 1, while stable regions such as Central North America (Nuttli, 1982; Singh and Herrmann, 1983) are characterized by lower values. The inferred dependency for central France lies again between the values typical of active and stable regions. Souriau *et al.* (1980) have measured the attenuation in the Massif Central at a larger period using Rayleigh waves. They obtained a value of 43 for  $Q$  at 50 sec. A direct extrapolation of our results yields a value surprisingly close:  $Q = 41$ . The minimum of  $Q$  around 0.5 to 1 Hz found in some regions (Aki, 1980; Biswas and Aki, 1984) is absent from our results.

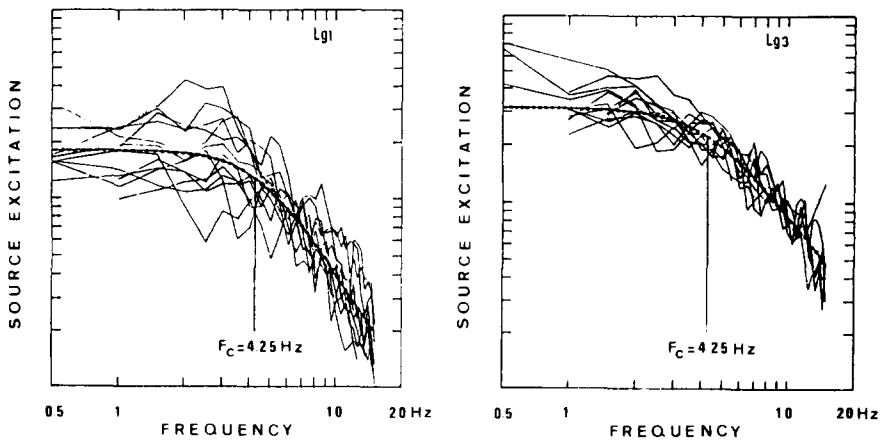


FIG. 12. Source excitation spectra obtained from the phases  $Lg1$  and  $Lg3$ .

The knowledge of the spectral energy decay can be used to retrieve the source excitation of each earthquake. As an example of this use of  $Lg$  waves, we present in Figure 12 the source spectra obtained from different stations (solid lines) from the phases  $Lg1$  and  $Lg3$ . The shapes of the spectra are similar in the two cases and lead to the same value of the corner frequency. The scattering of the results is smaller for the evaluation done with the  $Lg3$  phase which comprises the later arrivals of the  $Lg$  wavetrain. As we have shown, these waves heavily sample the lower crust which is probably the most homogeneous zone in the crust. The stronger scattering of the source spectra obtained from  $Lg1$  could be due to the higher sensitivity of this phase to near-surface heterogeneities.

### CONCLUSIONS

We have combined data analysis and numerical modeling to evaluate the mean quality factor of shear waves in the crust beneath central France.  $Q$  has been shown to be frequency-dependent in the form

$$Q(f) = 290 * f^{0.52}$$

for the most energetic part of the *Lg* wavetrain. We have illustrated by ray tracing some of the features of the *Lg* waves. This phase consists of multiply reflected waves trapped within the crust. Depending on the take-off angle and on the source depth, rays can be trapped in different regions of the crust. The sensitivity of *Lg* waves to a low *Q* zone is thus very different if this zone is located in the sediments or in the lower crust. The later arrivals are most sensitive to the attenuation in the lower crust. Experimental results indicate that the lower crust beneath central France is associated with a high value of *Q*.

Our results are compatible with the interpretation of the frequency dependence of *Q* as a tectonic indicator: stable regions are associated with *Q* which are monotonic and weakly increasing with frequency while, as pointed out by Aki (1980), active tectonic regions show a minimum of *Q* for frequencies around 0.5 to 1 Hz which implies a stronger increase of *Q* with frequency as predicted by the theoretical works of Sato (1984).

#### ACKNOWLEDGMENTS

We thank Dr. C. Y. Wang, Saint Louis University, for his comments on the high-frequency content of the *Lg* waves. This work was supported by the Advanced Research Projects Agency and was monitored by the Air Force Office of Scientific Research under Grant 80-0082.

#### REFERENCES

- Aki, K. (1980). Attenuation of shear waves in the lithosphere for frequencies from 0.05 to 25 Hz, *Phys. Earth. Planet. Interiors* **21**, 50–60.
- Aki, K. and B. Chouet (1975). Origin of coda waves: source, attenuation and scattering effects, *J. Geophys. Res.* **80**, 3322–3342.
- Bache, T. C., H. J. Swanger, B. Shkoller, and S. M. Day (1981). Simulation of short period *Lg*, expansion of three dimensional source simulation capabilities and simulation of near-field ground motion from the 1971 San Fernando, California earthquake, Final Report, Systems, Science and Software, La Jolla, California.
- Báth, M. and S. Crampin (1965). Higher modes of seismic surface waves—Relations to channel waves, *Geophys. J. R. Astr. Soc.* **9**, 309–321.
- Biswas, N. N. and K. Aki (1984). Characteristics of coda waves: central and southcentral Alaska, *Bull. Seism. Soc. Am.* **74**, 493–507.
- Bollinger, G. A. (1979). Attenuation of the *Lg* phase and the determination of  $m_b$  in the southeastern United States, *Bull. Seism. Soc. Am.* **69**, 45–63.
- Bouchon, M. (1981). A simple method to calculate Green's functions for elastic layered media, *Bull. Seism. Soc. Am.* **71**, 959–971.
- Bouchon, M. (1982). The complete synthesis of seismic crustal phases at regional distances, *J. Geophys. Res.* **87**, 1735–1741.
- Campillo, M., M. Bouchon, and B. Massinon (1984). Theoretical study of the excitation, spectral characteristics and geometrical attenuation of regional seismic phases, *Bull. Seism. Soc. Am.* **74**, 79–90.
- Herrmann, R. B. and A. Kijko (1983). Modeling some empirical vertical component *Lg* relations, *Bull. Seism. Soc. Am.* **73**, 157–171.
- Kennett, B. L. N. (1983). *Seismic Wave Propagation in Stratified Media*, Cambridge University Press, Cambridge, England.
- Mitchell, B. J. (1975). Regional Rayleigh wave attenuation in North America, *J. Geophys. Res.* **80**, 4904–4916.
- Mitchell, B. J. (1980). Frequency dependence of shear wave internal friction in the continental crust of eastern North America, *J. Geophys. Res.* **85**, 5212–5218.
- Mitchell, B. J. (1981). Regional variation and frequency dependence of *Q* in the crust of the United States, *Bull. Seism. Soc. Am.* **71**, 1531–1538.
- Muller, G. and S. Mueller (1979). Travel time and amplitude interpretation of crustal phases on the refraction profile DELTA-W, Utah, *Bull. Seism. Soc.* **69**, 1121–1132.
- Nicolas, M., B. Massinon, P. Mechler, and M. Bouchon (1982). Attenuation of regional phases in western Europe, *Bull. Seism. Soc. Am.* **72**, 2089–2106.



- Nuttli, O. W. (1973). Seismic wave attenuation and magnitude relations for eastern North America, *J. Geophys. Res.* **78**, 876–885.
- Nuttli, O. W. (1980). The excitation and attenuation of seismic crustal phases in Iran, *Bull. Seism. Soc. Am.* **70**, 469–485.
- Nuttli, O. W. (1981). On the attenuation of *Lg* waves in western and central Asia and their use as a discriminant between earthquakes and explosions, *Bull. Seism. Soc. Am.* **71**, 249–261.
- Nuttli, O. W. (1982). The earthquake problem in the eastern United States, *ASCE J. Struct. Div.* **108**, 1302–1312.
- Olsen, K. H., L. W. Braile, and J. N. Stewart (1983). Modeling short-period crustal phases (*P-Lg*) for long-range refraction profiles, *Phys. Earth Planet. Interiors* **31**, 334–347.
- Perrier, G. and J. C. Ruegg (1973). Structure profonde du Massif Central Français, *Ann. Geophys.* **29**, 435–502.
- Pomeroy, P. W. and T. C. Chen (1980). Regional seismic wave propagation, Final Report, Rondout Associates Inc., Stone Ridge, New York.
- Roecker, S. W., B. Tucker, J. King, and D. Hatzfeld (1982). Estimate of *Q* in central Asia as a function of frequency and depth using the coda of locally recorded earthquakes, *Bull. Seism. Soc. Am.* **72**, 129–149.
- Sato, H. (1979). Wave propagation in one dimensional inhomogeneous media, *J. Phys. Earth* **27**, 455–466.
- Sato, H. (1984). Attenuation and envelope formation of three-component seismograms of small local earthquakes in randomly inhomogeneous lithosphere, *J. Geophys. Res.* **89**, 1221, 1241.
- Singh, S. and R. B. Herrmann (1983). Regionalization of crustal coda *Q* in the continental United States, *J. Geophys. Res.* **88**, 527–538.
- Singh, S. K., R. J. Apsel, J. Fried, and J. N. Brune (1982). Spectral attenuation of *SH* waves along the Imperial fault, *Bull. Seism. Soc. Am.* **72**, 2003–2016.
- Souriau, A., A. M. Correig, and M. Souriau (1980). Attenuation of Rayleigh waves across the volcanic area of the Massif Central, France, *Phys. Earth Planet. Interiors* **23**, 52–71.
- Thouvenot, F. (1983). Frequency dependence of the quality factor in the upper crust: a deep seismic sounding approach, *Geophys. J. R. Astr. Soc.* **73**, 427–447.

LABORATOIRE DE GÉOPHYSIQUE INTERNE  
ET TECTONOPHYSIQUE U.A. CNRS 733, IRIGM  
UNIVERSITÉ DE GRENOBLE  
BP 68, 38402 SAINT MARTIN D'HERES  
CEDEX, FRANCE (M.C., M.B.)

LABORATOIRE DE DÉTECTION GÉOPHYSIQUE  
COMMISSARIAT À L'ÉNERGIE ATOMIQUE  
BP 12, 91680 BRUYERE-LE-CHATEL,  
FRANCE (J.L.P.)

Manuscript received 12 December 1984